An Experimental and Theoretical Framework for Manufacturing Prosthetic Sockets for Transtibial Amputees

Mario C. Faustini, Richard R. Neptune, Richard H. Crawford, William E. Rogers, and Gordon Bosker

***Abstract*—Selective laser sintering (SLS) is a powerful manufacturing technology that does not require part-specific tooling or significant human intervention and provides the ability to easily generate parts with complex geometric designs. The present work focuses on developing a manufacturing framework using this technology to produce subject-specific transtibial amputee prosthetic sockets made of Duraform PA, which is a nylon-based material. The framework includes establishing an overall socket design (using the patellar-tendon bearing approach), performing a structural analysis using the finite element method (FEM) to ensure structural reliability during patient use, and validating the results by comparing the model output with experimental data. The validation included quantifying the failure conditions for the socket through a series of bending moment and compression tests. In the case study performed, the FEM results were within 3% of the experimental failure loads for the socket and were considered satisfactory.**

***Index Terms*—Finite element methods (FEM), prosthetic sockets, software prototyping, transtibial amputees.**

I. Introduction

FOR lower extremity amputees, a well-fitting socket is an important element for a successful rehabilitation [1]. The socket provides the interface between the prosthesis and residual limb, which is designed to provide comfort, appropriate load transmission, and efficient movement control. Attaining these objectives is extremely challenging, with up to 55% of lower limb amputees reporting dissatisfaction with socket comfort, residual limb pain, and/or skin breakdown [1], [2]. In addition, current techniques used to produce sockets with suitable characteristics are labor and cost intensive, and depend on the work of skilled prothetists that are relatively scarce compared to the number of lower limb amputees. Currently, there are more than 500 000 lower limb amputees in the U.S. alone, with 60 000 new ones every year [1]. Thus, an objective and systematic framework for fabricating prosthetic sockets would help improve efficiency in prosthetic care, reduce time and cost to improve amputee rehabilitation, and potentially enhance comfort and fit. Previous systematic approaches have been limited in the scientific literature, and either have not focused on the engineering design and structural analysis of the socket or included an experimental validation of the structural analysis (e.g., [3], [4]).

An effective technology that would allow for a systematic approach is selective laser sintering (SLS), which is a versatile manufacturing technique with several advantages over traditional methods [5]–[8]. First, SLS can directly create sockets from digital subject-specific shape information, which eliminates the need for molds, hand lamination and finishing procedures. Second, SLS has the ability to create complex geometries with minimal cost penalty in manufacturing. From a design perspective, this significantly expands the options for developing and exploring alternate socket designs, including geometric variants of traditional socket shapes, and for incorporating compliant features in selected locations to relieve high contact pressure at the limb–socket interface. Third, the integration of additional prosthetic components and features directly into the socket is straightforward (e.g., an integrated pylon mounting system).

The overall goal of this research was to develop a framework consisting of a systematic manufacturing technique to produce subject-specific sockets made of Duraform PA material using SLS. The elements of the framework include obtaining a digital image of the patient's limb and defining the overall socket design using the patellar-tendon bearing approach, performing a structural analysis using the finite element method (FEM) to ensure structural reliability during patient use, and validating the FEM results with experimental data. To assess the effectiveness of the framework, a case study was performed.

II. Methods

The socket design and fabrication framework includes the following steps (Fig. 1): 1) surface model development using the geometry of the residual limb acquired through laser scanning, 2) computer-aided design model development using appropriate design constraints, 3) FEM analysis of the socket using related boundary conditions, 4) SLS fabrication, and 5) an experimental validation of the FEM analysis results. These steps are described in detail below.

A. Surface Model Development

The first step is to acquire the patient's residual limb shape information through laser scanning of the residual limb or a positive mold cast directly from the patient's limb. For the case

Manuscript received July 18, 2005; revised December 22, 2005; accepted May 23, 2006. This work was supported under VA Research and Development Grant A2755-r. The work of M. C. Faustini was support by the National Council for Scientific and Technological Development (CNPq) Fellowship #200063/99-5.

M. C. Faustini, R. R. Neptune, and R. H. Crawford are with the Department of Mechanical Engineering, The University of Texas, Austin, TX 78712-0292 USA (e-mail: rneptune@mail.utexas.edu).

W. E. Rogers and G. Bosker are with the Department of Rehabilitation Medicine, The University of Texas Health Science Center, San Antonio, TX 78229-3900 USA.

Digital Object Identifier 10.1109/TNSRE.2006.881570

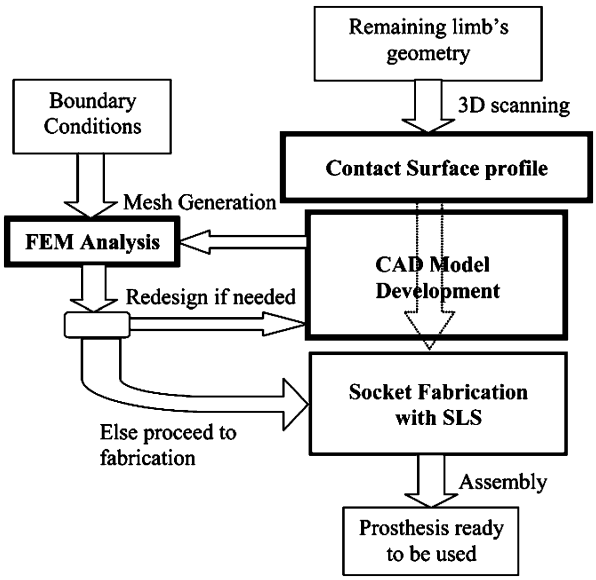

Fig. 1. Framework for subject-specific socket design, analysis and manufacturing.

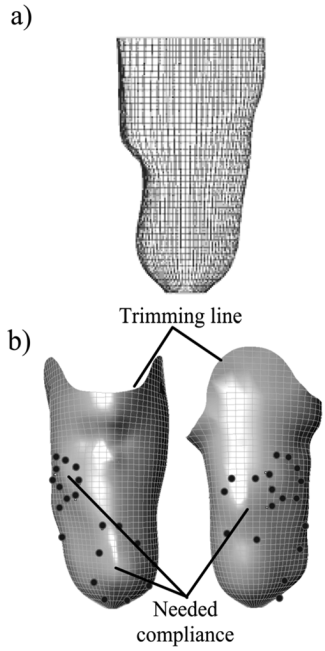

Fig. 2. a) Laser scanned surface model of residual limb. b) Rectified and trimmed inner surface for the socket with points marking areas identified by the prosthetist where compliance is desired.

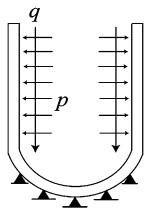

Fig. 3. Load diagram used for initial estimation of wall thickness based on a thin-walled cylinder approximation for the socket shape. Wall thickness was evaluated using contact pressure (q) and shear stress (p) data taken from the literature.

study, a positive mold of an active 54-year-old male (height, 1.68 m; mass 65 kg) who was free from any musculoskeletal disorders and had been a transtibial traumatic amputee for 23 years was scanned. A Seattle Limb Systems ShapeMaker 3000 (Poulsbo, WA) laser scanner was used to provide the point cloud data that described the limb shape with an angular resolution of 3° and a linear resolution of 3 mm. The point cloud was converted to a surface model [Fig. 2(a)] that was then used by the prosthetist to define the appropriate trim line at the top of the socket and rectifications for a patella-tendon bearing socket design (PTB) [9], [10]. GordoScan software (UTHSCSA, San Antonio, TX) was used to perform the rectifications. The surface model was also used by the prosthetist to indicate areas of needed compliance to help reduce socket–limb interface pressure [Fig. 2(b)]. At this stage, the surface model described precisely the desired socket inner shape (based on the prosthetist's feedback) and was ready for the subsequent engineering design and analysis.

B. Design Constraints

The primary design constraint was to preserve the subject-specific inner shape of the surface model. Additional design considerations included minimizing the weight of the socket, adding area-specific compliance to relieve socket–limb interface pressure and maintaining appropriate strength to withstand the normal loads experienced during human gait. In addition, aesthetic considerations to produce a socket shape that mimics the profile of the leg anatomy were also important. The overall topology of a traditional thin-walled shell socket satisfied this set of design constraints.

C. Socket CAD Model Development

The next step was to create a solid model of the socket by adding thickness to the surface model (Fig. 1: computer-aided design (CAD) model development). The initial calculation for the socket wall thickness was estimated using a thin-walled cylinder as an approximation (Fig. 3). The radius of the cylinder was estimated using the mean radius of the inner surface, and the contact pressure and shear stress were estimated using the peak values found in the literature [11]–[13].

The equation used to define the overall thickness of the socket wall is given by [14], [15]

$$t = \frac{qR^2 + \frac{p}{2}\nu RL}{E\Delta R_{\max}} \tag{1}$$

where q is the normal pressure load, p is the transferred shear stress, ν is Poisson's ratio, R is the radius of the cylinder, L is the cylinder length, E is Young's modulus, and $\Delta R_{\max}$ is the maximum desired radial expansion. An overall cylinder radius expansion of 1% or less under load was considered an acceptable strain for the goal of maintaining socket fit.

To ensure the structural integrity of the socket, the resulting wall thickness t was designed such that the stresses do not exceed the material strength

$$S_y > p + \frac{qR}{t} \tag{2}$$

where S_y is the value for tensile strength of SLS Duraform PA material, q is the contact pressure, p is the shear stress, and R is the socket radius. Once the appropriate initial value for wall thickness was identified using (1), the inner surface profile was modified using CAD software (Rhinoceros 3D, Robert McNeel & Associates, Seattle, WA) to produce the final socket shape using a multistep process. First, an "outwards" offset operation was applied to the inner surface of the socket. Then, a "blend" operation was performed at the top free edges of the inner surface and offset surface to transform the model into a closed solid model.

At this point, additional design features were added to finalize the design, including the geometry to facilitate the pylon attachment to the bottom of the model using our previously described approach [16]. In addition, we were also interested in adding compliant features to relieve contact pressure [Fig. 2(b)], which were implemented using reduced wall thickness at designated sites. This was performed using "offset" operations on the outer surface sections surrounding the sites identified by the study prosthetist. Once these sections were defined, they were rejoined to the overall outer surface using "blend" operations, which preserved the model as a closed volume. The structural integrity of the wall thickness was refined through iterative FEM analyses of these compliant sections using the desired deformation defined by the prosthetist as the design objective.

D. FEM Analysis

In order to evaluate the structural behavior of the socket under expected applied loads, a FEM model was created from the socket CAD model (Fig. 1, FEM analysis) using I-deas (EDS, Plano, TX). The socket CAD model was imported into I-deas using the IGES file format. A Delaunay-based [17] mesh generator was used to create the initial model mesh. The elements used were ten-node parabolic tetrahedra, and the initial element size was chosen to be less than the overall socket wall thickness. The automated mesh generator was set to create a model based on sections, which allowed specific areas and geometric features to be further refined. The resulting mesh was interactively inspected to identify highly distorted or stretched elements that might lead to errors in the analysis. When such areas were identified, individual elements were locally refined. The complete FEM mesh for the socket had a total of 7582 elements and 22 570 nodes.

The SLS material used in this study was Duraform PA [18], which is a type of nylon that has material properties suitable for prosthetic sockets (Table I).

E. Load Conditions

The socket FEM analysis was performed under different loading and boundary conditions in order to evaluate the structural integrity of the socket during normal walking conditions. First, a simulation was run to analyze the behavior of the socket under the peak limb-socket pressure profile and shear stresses found in the literature for individuals with a similar body weight as our case study [19]–[22]. These measured values were then applied to the socket as boundary conditions on the inner socket surface where the contact occurs. Values for contact pressure and shear stress were defined at ten areas: the medial and lateral tibial supracondyles, medial and lateral tibia, medial and lateral gastrocnemius, patellar tendon, popliteal depression, distal tibia and fibula head (Fig. 4). Also, a zero load condition was applied to the top edge of the inner surface. In order to produce a smooth continuous pressure distribution at the contact surfaces, a refined inverse distancing interpolation algorithm was used (see the Appendix).

Once the load values were constructed and applied to the elements of the socket inner surface, the pylon attachment fitting features at the socket bottom were spatially restrained. The resulting stresses obtained from the FEM analysis were then used to assess the socket structural integrity by comparing the stresses with the ultimate tensile strength of the SLS material.

F. SLS Fabrication

To validate the FEM analysis results, prototypes of the socket were manufactured using SLS (Fig. 5). The socket CAD

TABLE I
MATERIAL PROPERTIES FOR DURAFORM PA

Property	Value
Tensile strength	44 MPa
Tensile modulus	1600 MPa
Flexural modulus	1285 MPa
Melting Point	184°C
Tensile Elongation at Break	9%
Impact Strength (Notched Izod)	214 J/m

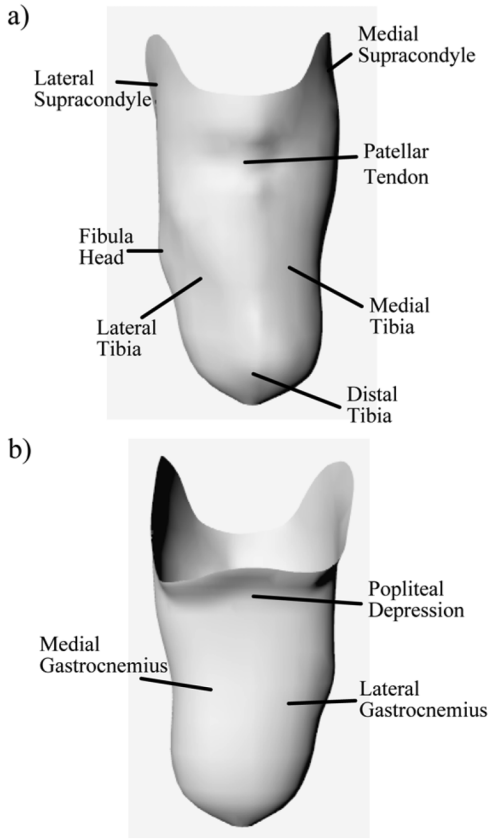

Fig. 4. a) Anterior and b) posterior views of the inner socket profile displaying the points used in the definition of the pressure distribution boundary condition.

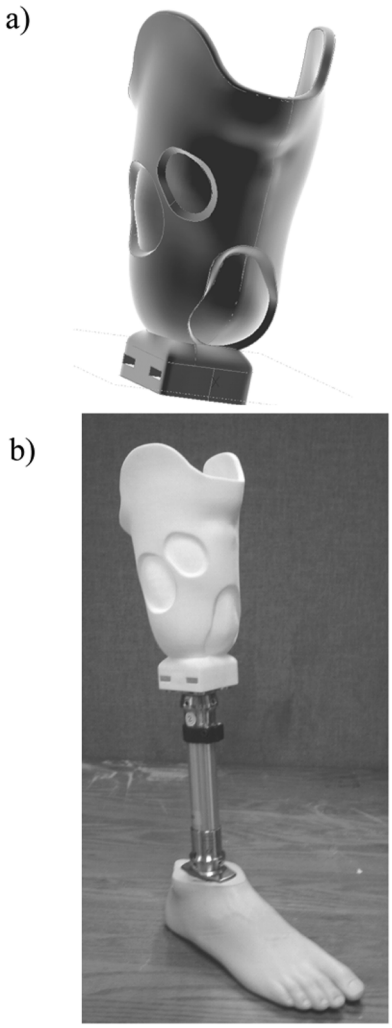

Fig. 5. a) Final CAD model of the socket. b) Ready-to-wear prosthesis with the SLS produced Duraform PA Socket.

model was exported using the STL format, which is a standard format for SLS systems (Fig. 1: socket fabrication). SLS is a manufacturing technique that fabricates any closed solid model in sequential cross-sectional layers. A planar layer of material powder is placed in the part bed and sintered or melted in the desired cross section of the model by a high-powered laser beam and is then allowed to solidify. The bed is then lowered by one layer thickness and covered with another layer of material powder and the process is repeated. When all the cross sections of the model are processed, the final socket possesses the same shape and dimensions as the computer model.

The sockets in the present case study were produced using a Sinterstation 3500 (3D Systems, Valencia, CA). Two identical sockets were fabricated for the experimental validation in a vertical position for optimal sintering and thermal conditions. The total fabrication time and Duraform PA material costs for both sockets, when fabricated simultaneously, including the warm up and cool down phases, was 15 h and $527, respectively, during which the machine operated completely unassisted. The sinterstation could manufacture up to four sockets of the size in the present study simultaneously with no increase in time

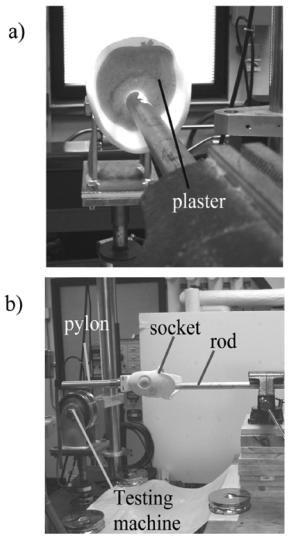

Fig. 6. a) Top view of the socket filled with plaster and a rod located in the middle to apply the loads. b) Experimental setup for the simulated heel strike test.

or material cost. The tolerance of the fabricated socket profiles followed the typical accuracy of SLS fabricated parts using Duraform, which is ± 0.25 mm. Once the fabrication was finished, the sockets were ready to be assembled with a pylon and foot–ankle components.

G. Experimental Validation

In order to validate the FEM socket model, we developed two experiments to assess the structural responses of the socket and compare them with FEM predictions generated with boundary conditions similar to the experimental conditions. The first experiment simulated the maximum bending moment observed during a heel strike (Fig. 6) [23]. The socket was filled with sand and plaster with a steel rod placed in the center. Once the plaster cured, the pylon and attachment were mounted to the bottom of the socket. The entire assembly was placed in a horizontal position, with the end of the rod firmly gripped by a vise attached to a fixed table. The end of the pylon was positioned in a hydraulic testing machine (MTS Systems Corporation, Eden Prairie, MN). The piston of the hydraulic machine applied a gradually increasing perpendicular force to the end of the pylon while a load cell and data acquisition system recorded the force magnitude and displacement. The bending moment was increased until the socket failed.

A second validation test assessed the maximum compressive force that could be applied to the inner surface of the socket and the resulting deformation at one of the compliant features. An initial pilot study was performed to demonstrate that the top of the socket could be modified into a cylindrical shape without significantly changing the stress and displacement distribution in the remainder of the socket [24]. This allowed us to modify the existing socket to have a cylindrical top so that the socket could be filled with a load-transferring medium while a piston applied a compressive force. With this verification, a top-modified socket was manufactured with all other dimensions preserved and filled with 1-mm-diameter zirconia-toughened alumina (ZTA) beads. This medium was chosen because it was

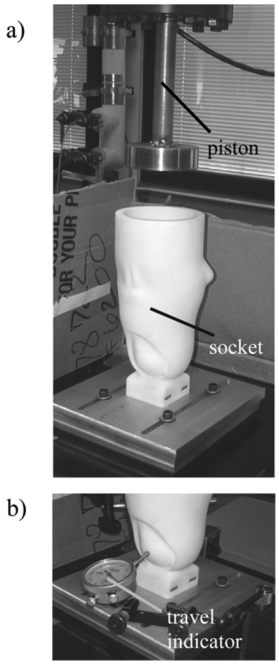

Fig. 7. a) Setup for compression test: socket attached to a hydraulic test machine and filled with ZTA medium to be compressed by the piston. b) Travel indicator to measure the deformation.

strong enough to withstand the high compressive force while minimizing the effects of friction. This created a uniform pressure distribution over the entire inner surface of the socket that could be replicated using appropriate boundary conditions in the FEM model. The hydraulic testing machine was then used to gradually compress the medium with a piston until the socket failed [Fig. 7(a)]. A travel indicator was used to measure the deformation of the socket wall at the bottom compliant feature [Fig. 7(b)] as the applied load increased.

III. Results

The FEM analysis of the stresses within the socket under peak pressure and shear stress loading conditions that would be experienced during walking (Fig. 8) revealed that the maximum stress occurred at the bottom of the socket (42.5 MPa) and was within the material tolerance of Duraform PA (44 MPa). For the simulated heel-strike validation test, the FEM simulation predicted that the socket would fail when the applied perpendicular force exceeded 690 N and produced a stress value of 45.2 MPa, which was just above the failure stress of Duraform PA (44 MPa). During the experimental simulated heel-strike test, the socket failed with an applied force of 710 N, which was within 3% of the FEM predicted value. In addition, the socket failed in the region where the FEM analysis predicted the peak stress would occur (Fig. 9).

The compression test revealed that the force at failure was 26.3 kN, which was nearly identical to the force (26.5 kN) predicted by the FEM analysis [Fig. 10(a)]. This peak force produced a maximum stress of 45.3 MPa, which was just above the failure stress of Duraform PA (44 MPa). The measured orthogonal deformation at the bottom compliant feature was found to be within 25% of the values predicted by the FEM for all loads less than 78% of the failure force [Fig. 10(b)].

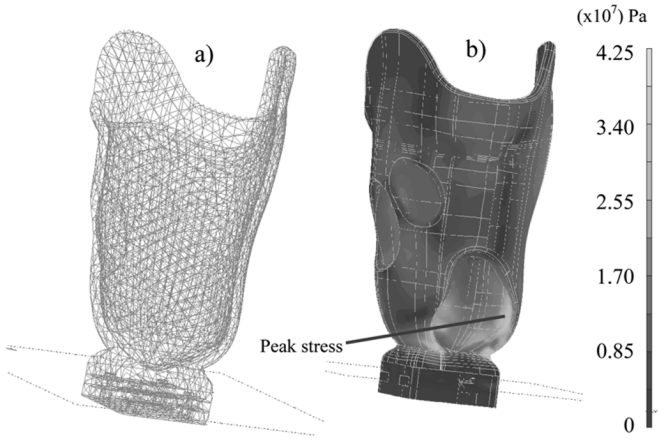

Fig. 8. a) FEM model of the socket. b) FEM results for stresses under peak loading conditions measured during normal walking (in Pascal).

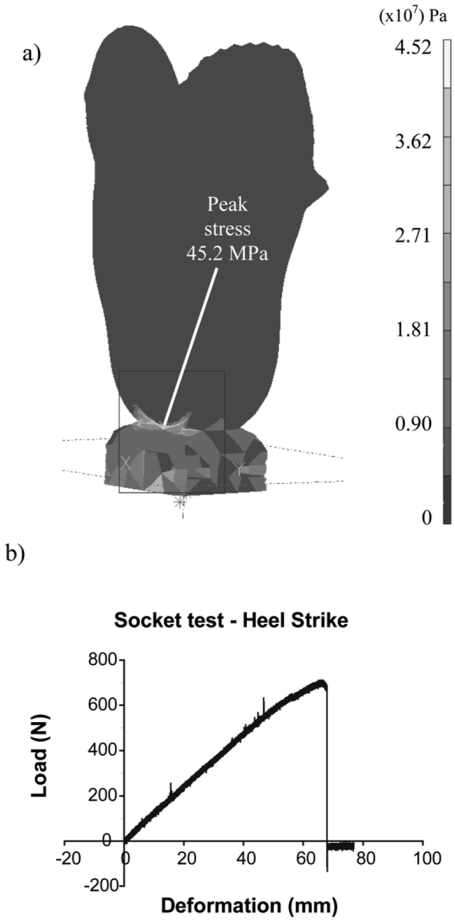

Fig. 9. a) FEM results for the stresses in the socket with bending moment boundary conditions (in Pascal). b) Output from the MTS machine, showing the load applied at the pylon versus the corresponding displacement during the simulated heel strike test.

IV. Discussion

The purpose of this study was to present an objective and systematic framework for producing subject-specific prosthetic sockets for transtibial amputees using SLS (Fig. 1). The framework included the acquisition of the residual limb shape through laser scanning, a methodology for socket design, structural analysis using FEM to ensure structural reliability under normal

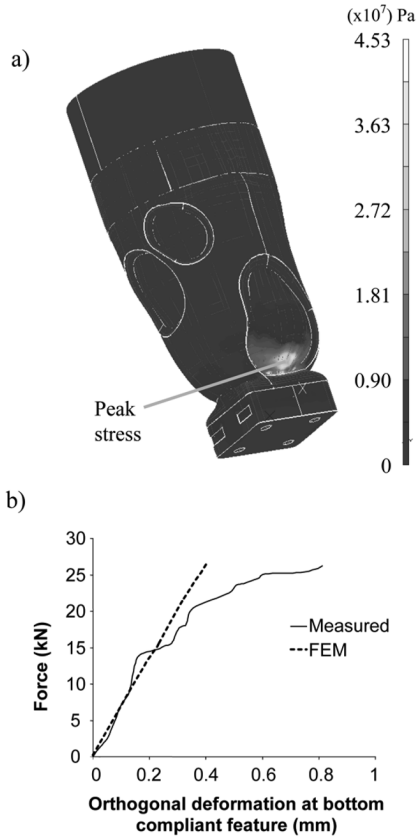

Fig. 10. a) FEM results for the stresses in the socket with a compressive force boundary condition (in Pascal). b) Comparison between measured deformation at bottom of compliant socket with FEM results.

loads observed during walking, and socket fabrication using SLS. A case study was performed using experimental tests of the SLS sockets manufactured via the framework to provide validation of the FEM analysis. The results of the validation were very promising, with the FEM predictions for failure loads in both tests within 3% of measured values. For the compression test deformation data, the predictions were within 25%, but only for loads under 78% of the failure load. For values above this threshold, discrepancies between the predicted and measured results occurred due to the transition of the socket model into a large deformation regime, which cannot be accurately captured using the current FEM model. To improve the accuracy during such situations, a more refined FEM mesh would be necessary, in addition to a material characterization of the nonlinear behavior of Duraform PA during large deformations. Such material characterization remains as an area of future work.

A limitation of the present FEM analysis was the determination of the pressure profile applied to the prosthesis, which can greatly vary among patients (e.g., [10], [21], [22], [25]). Ideally, the pressure profile should be measured in the actual socket being analyzed to ensure the loading conditions are precise. However, obtaining actual pressure measurements from each socket iteration is not feasible. Furthermore, previous analysis has shown that instrumenting a socket for contact pressure measurement may considerably change the interface conditions from their normal state [26]. However, a promising alternative is to assess the load transfer directly from a FEM model of the residual limb, including the bones, soft tissues and liner (e.g., [10], [17], [20]), where the dimensional data to generate the corresponding meshes come from computed tomography (CT) or magnetic resonance imaging (MRI) scans. Current work is being directed at integrating such FEM models to obtain pressure data for the design analysis.

Although the present framework provides a satisfactory means for prosthetists to produce effective, subject-specific sockets, the current framework involves many steps that require experience using CAD and FEM analysis software. Future work should be directed at providing an integrated user-friendly system that automates many of the CAD operations needed to produce the solid model of the socket, including wall thickening and incorporating compliant features and pylon attachment fittings.

One final area of future work is to assess the effect of dynamic transient and impulsive loading conditions on the structural integrity and durability of the socket. This will require additional experimentation and the determination of the fatigue properties of Duraform PA and other SLS materials.

One main advantage of the present framework is that it allows for systematic and controlled design modifications in the socket shape or volume, which allows the exploration of the relative advantages of various socket design philosophies (e.g., PTB versus total surface bearing, smooth versus abrupt contouring of socket features) [9], [27]. A second advantage is that compliant features can be easily integrated into the socket design. The present design integrated one form of compliance (i.e., thin-walled sections) and future work will examine other forms of compliant features. Finally, the FEM analysis indicated that the largest stress concentration occurred at the bottom of the socket near the pylon attachment site. Thus, with our framework, we would modify the design to remove the stress concentration in that area and ensure an appropriate factor of safety for the entire socket. This is one of the more powerful aspects of such a framework, that design iterations can be performed before a socket is manufactured to ensure a structurally sound design and provide long-term reliability.

APPENDIX

The pressure distribution functions that define the data surfaces used as boundary conditions (Section II-E) were generated through refined inverse distancing, and the algorithm was mathematically defined as follows.

Given a set of pressure values $p_1, \ldots, p_n$ at n discreet points $\mathbf{P}_1, \ldots, \mathbf{P}_n$ on a parametric surface $\mathbf{S}(u, v)$ of the socket model, create for each discrete point $\mathbf{P}_i$ a local interpolation function

$$Q_i = p_i + a_1 (u - u_i)^2 + a_2 (u - u_i)(v - v_i) + a_3 (v - v_i)^2 + a_4 (u - u_i) + a_5 (v - v_i) \quad (3)$$

where u_i and v_i are the parametric coordinates of $\mathbf{P}_i$ and $a_1, \ldots, a_5$ are the pressure values at the five points of the set $\mathbf{P}_1, \ldots, \mathbf{P}_n$ that are closest to $\mathbf{P}_i$.

Also, for each discrete point $\mathbf{P}_i$, calculate a weighting factor

$$W_i = \frac{r_i - d_i}{(r_i \cdot d_i)^2} \quad (4)$$

where r_i is the radius of influence in the parametric space (u, v) around point $\mathbf{P}_i$ (defined to be equal to 0.05) and d_i is the parametric distance between (u, v) and (u_i, v_i).

Thus, the resulting continuous pressure distribution on the surface $S(u, v)$ is defined by

$$p(u,v) = \frac{\sum_{i=1}^{n} W_i Q_i}{\sum_{i=1}^{n} W_i}. \quad (5)$$

REFERENCES

[1] W. E. Rogers, R. H. Crawford, J. J. Beaman, and N. E. Walsh, "Fabrication of prosthetic sockets by selective laser sintering," in *Proc. 1991 Solid Freeform Fabrication Symp.* , Austin, TX, Aug. 12–14, 1991, pp. 158–163.

[2] B. Rogers, A. Gitter, G. Bosker, M. Faustini, M. Lokhande, and R. Crawford, "Clinical evaluation of prosthetic sockets manufactured by selective laser sintering," in *Proc. 12th Solid Freeform Fabrication Symp.*, Austin, TX, Aug. 6–8, 2001, pp. 505–512.

[3] S. G. Zachariah, J. E. Sanders, and G. M. Turkiyyah, "Automated hexahedral mesh generation, from biomedical image data: Applications in limb prosthetics," *IEEE Trans. Rehabil. Eng.*, vol. 4, no. 2, pp. 91–102, Jun. 1996.

[4] M. B. Silver-Thorn, "Prediction and experimental verification of residual limb-prosthetic socket interface pressures for below-knee amputees," Ph.D. dissertation, Northwestern University, Evanston, IL, 1991.

[5] N. E. Walsh, J. L. Lancaster, V. W. Faulkner, and W. E. Rogers, "A computerized system to manufacture prostheses for amputees in developing countries," *J. Prosthetics Orthotics*, vol. 1, no. 3, pp. 165–181, 1989.

[6] D. Freeman and L. Wontorcik, "Stereolithography and prosthetic test socket manufacture: A cost/benefit analysis," *J. Prosthetics Orthotics*, vol. 10, no. 1, pp. 17–20, 1998.

[7] W. Rogers, A. Gitter, G. Bosker, M. Faustini, M. Lockhande, and R. Crawford, "Clinical evaluation of prosthetic sockets manufactured by selective laser sintering," presented at the Solid Freeform Fabrication Symp., Austin, TX, 2001.

[8] M. Faustini, R. Crawford, W. Rogers, A. Gitter, and G. Bosker, "Finite element structural analysis of prosthesis sockets for below-the-Knee amputees manufactured by SLS," presented at the Solid Freeform Fabrication Symp., Austin, TX, 2001.

[9] J. Fergason and D. G. Smith, "Socket considerations for the patient with a transtibial amputation," *Clin. Orthopaedics Related Res.*, no. 361, pp. 77–86, 1999.

[10] M. Zhang and C. Roberts, "Comparison of computational analysis with clinical measurement of stresses on below-knee residual limb in a prosthetic socket," *Med. Eng. Phys.*, no. 22, pp. 607–612, 2000.

[11] J. E. Sanders, S. G. Zachariah, A. B. Baker, J. M. Greve, and C. Clinton, "Effects of changes in cadence, prosthetic componentry, and time on interface pressures and shear stresses of three trans-tibial amputees," *Clin. Biomech.*, no. 15, pp. 684–694, 2000.

[12] M. Zhang, A. Mak, and V. C. Roberts, "Finite element modeling of residual lower-limb in a prosthetic socket: A survey of the development in the first decade," *Med. Eng. Phys.*, no. 20, pp. 360–373, 1998.

[13] M. Zhang, A. R. Turner-Smith, V. C. Roberts, and A. Tanner, "Frictional action at lower limb/prosthetic socket interface," *Med. Eng. Phys.*, vol. 18, no. 3, pp. 207–214, 1996.

[14] R. J. Roark and W. C. Young, *Formulas for Stress and Strain*. New York: McGraw-Hill, 1975.

[15] W. D. Pilkey, *Formulas for Stress, Strain, and Structural Matrices*. New York: Wiley, 1994.

[16] D. Burhan, "Redesign attachment fitting of transtibial prosthetic socket using selective laser sintering," M.S. thesis, Univ. Texas, Austin, 2004.

[17] S. Zachariah and J. E. Sanders, "Interface mechanics in lower-limb external prosthetics: A review of finite element models," *IEEE Trans. Rehabil. Eng.*, vol. 4, no. 4, pp. 288–302, Dec. 1996.

[18] Materials for SLS systems: Datasheet for duraform PA and GF, 3DSystems 2004 [Online]. Available: http://www.3dsystems.com/products/datafiles/lasersintering/datasheets/DURAFORMHigh.pdf

[19] M. Faustini, "Modeling and fabrication of prosthetic sockets using selective laser sintering," Ph.D. dissertation, Univ. Texas, Austin, 2004.

[20] W. C. C. Lee, M. Zhang, X. Jia, and J. T. M. Cheung, "Finite element modeling of the contact interface between trans-tibial residual limb and prosthetic socket," *Med. Eng. Phys.*, no. 26, pp. 655–662, 2004.

[21] J. E. Sanders and C. H. Daly, "Interface pressures and shear stresses: Sagittal plane angular alignment effects in three trans-tibial amputee case studies," *Prosthetics Orthotics Int.*, no. 23, pp. 21–29, 1999.

[22] M. Zhang, A. R. Turner-Smith, A. Tanner, and V. C. Roberts, "Clinical investigation of the pressure and shear stress on the trans-tibial stump with a prosthesis," *Med. Eng. Phys.*, no. 20, pp. 188–198, 1998.

[23] A. Brooks, "Bending Strength Test and Evaluation of a Transtibial Prosthetic Socket Fabricated by Selective Laser Sintering," M.S. thesis, The University of Texas at Austin, , 2004.

[24] V. S. Dixit, "Compression test of trans-tibial prosthesis sockets using granular media boundary condition," M.S. thesis, Univ. Texas, Austin, 2004.

[25] J. E. Sanders, J. M. Greve, C. Clinton, and B. J. Hafner, "Changes in interface pressure and stump shape over time: preliminary results from a trans-tibial amputee subject," *Prosthetics Orthotics Int.*, no. 24, pp. 163–168, 2000.

[26] A. F. T. Mak, M. Zhang, and D. A. Boone, "State-of-the-art research in lower-limb prosthetic biomechanics-socket interface," *J. Rehabil. Res. Devel.*, vol. 38, no. 2, Mar./Apr. 2001.

[27] J. Kahle, "Conventional and hydrostatic transtibial interface comparison," *J. Prosthetics Orthotics*, vol. 11, no. 4, pp. 85–91, 1999.

Mario C. Faustini received the B.S. degree in mechatronics engineering and the M.S.M.E. degree from the University of São Paulo, São Paulo, Brazil, in 1997 and 1999, respectively, and the Ph.D. degree from The University of Texas, Austin, in 2004.

Since 2004, he has been a Postdoctoral Fellow at The University of Texas, Austin. His research interests include development and application of computational tools in the design, analysis and simulation of prosthetics and orthotics, rehabilitation engineering, and the application of solid freeform fabrication techniques such as selective laser sintering.

Richard R. Neptune received the B.S., M.S., and Ph.D. degrees in mechanical engineering from the University of California, Davis, in 1991, 1993, and 1996, respectively. He completed a postdoctoral fellowship at the University of Calgary, Calgary, AB, Canada, from 1996 to 1998.

He then served as a Biomedical Engineer at the VA Palo Alto Rehabilitation Research and Development Center in Palo Alto, CA from 1998 to 2000. He is currently an Associate Professor with the Department of Mechanical Engineering at The University of Texas, Austin. His research interests include musculoskeletal modeling and simulation of human movement, prosthetic and orthotic design optimization, and neural control of movement.

Richard H. Crawford received the B.S.M.E. degree from Louisiana State University, Baton Rouge, in 1982 and the M.S.M.E. and Ph.D. degrees from Purdue University, West Lafayette, IN, in 1985 and 1989, respectively.

He is currently a Professor with the Department of Mechanical Engineering at The University of Texas, Austin. His research interests include development of computational representations and tools to support exploration of complex engineering design spaces and geometric processing, design tools, and manufacturing applications of solid freeform fabrication techniques such as selective laser sintering.

William E. Rogers received the B.S. and M.S. degrees in physics from the Trinity University, San Antonio, TX, in 1974 and 1981, respectively.

He is currently the Director of the Computer Laboratory of the Department of Rehabilitation Medicine, The University of Texas Health Science Center, San Antonio.

Gordon Bosker received the B.S. degree in industrial engineering from the Wichita State University, Wichita, KS, in 1979 and the C.P. degree from Northwestern University, Evanston, IL, in 1994.

Since 1998, he has been an Instructor with the Department of Rehabilitation Medicine, The University of Texas Health Science Center, San Antonio.